Temporomandibular joint formation requires two distinct hedgehog-dependent steps

Patricia Purcell[a,b], Brian W. Joo[a,b], Jimmy K. Hu[a], Pamela V. Tran[b], Monica L. Calicchio[c], Daniel J. O'Connell[b], Richard L. Maas[b], and Clifford J. Tabin[a,1]

[a]Department of Genetics, Harvard Medical School, Boston, MA 02115; [b]Division of Genetics, Department of Medicine, Brigham and Women's Hospital and Harvard Medical School, Boston, MA 02115; and [c]Department of Pathology, Children's Hospital Boston, Boston, MA 02115

Contributed by Clifford J. Tabin, August 10, 2009 (sent for review July 17, 2009)

We conducted a genetic analysis of the developing temporo-mandibular or temporomandi-bular joint (TMJ), a highly specialized synovial joint that permits movement and function of the mammalian jaw. First, we used laser capture microdissection to perform a genome-wide expression analysis of each of its developing components. The expression patterns of genes identified in this screen were examined in the TMJ and compared with those of other synovial joints, including the shoulder and the hip joints. Striking differences were noted, indicating that the TMJ forms via a distinct molecular program. Several components of the *hedgehog* (*Hh*) signaling pathway are among the genes identified in the screen, including *Gli2*, which is expressed specifically in the condyle and in the disk of the developing TMJ. We found that mice deficient in *Gli2* display aberrant TMJ development such that the condyle loses its growth-plate-like cellular organization and no disk is formed. In addition, we used a conditional strategy to remove *Smo*, a positive effector of the Hh signaling pathway, from chondrocyte progenitors. This cell autonomous loss of *Hh* signaling allows for disk formation, but the resulting structure fails to separate from the condyle. Thus, these experiments establish that Hh signaling acts at two distinct steps in disk morphogenesis, condyle initiation, and disk–condyle separation and provide a molecular framework for future studies of the TMJ.

Indian hedgehog | Gli2 | synovial joints | microarray

The temporomandibular joint (TMJ) is a complex structure that is essential for jaw movement and found only in mammals. Its major components include the glenoid fossa of the temporal bone, the condylar head of the mandible, and a fibrocartilaginous disk that is located between these bones, dividing the joint cavity into two compartments. Both the condyle and the glenoid fossa are endochondral in origin. The first evidence of TMJ formation during development is the appearance of distinct mesenchymal condensations, the temporal and condylar blastemas. The condylar blastema rapidly grows toward the temporal blastema, closing the gap between them while a distinct articular disk forms within the joint as a separate condensation (1).

The TMJ differs from most synovial joints in several ways. First, the TMJ forms by appositional growth, as opposed to segmentation of a continuous skeletal condensation. Second, in the TMJ, the articular surfaces of the condyle and glenoid fossa are covered by a layer of fibrous rather than hyaline cartilage. Last, the two bones are in contact with an intervening fibrocartilaginous disk rather than articulating with each other directly. The development of the TMJ during prenatal life also lags behind other joints in both the time of its initiation and its development. In the mouse, all of the major anatomical features of the TMJ, including the disk, are present by E16.5, although the condyle and glenoid fossa continue to increase in size and density into adulthood.

Although the structural features of the TMJ are well documented, little information is available with respect to the genetic, cellular, and molecular mechanisms involved in TMJ morphogenesis. In contrast, studies of other skeletal elements, most notably of the developing limb, have provided a wealth of information about signals involved in synovial joint formation. Most synovial joints develop by the cleavage or segmentation of a continuous skeletal condensation (2–4). The first morphological sign of joint formation is the appearance of a transverse stripe of cells, the interzone, a three-layered region with reduced cell density in the center that marks the area destined to become the joint space (5, 6). This morphological change is presaged by molecular events, including the down-regulation of several genes expressed in the remainder of the developing cartilage, such as *Sox9*, a member of the Sox family of transcription factors present in all chondroprogenitor cells (7, 8). Conversely, a large number of genes are induced specifically in the location of the future joint. Prominent among these are *Wnt9a* (formerly called *Wnt14*), a canonical Wnt ligand (9–11), and depending on the specific joint, *Gdf5*, *Gdf6*, or *Gdf7*, members of the BMP/TGFβ superfamily (12–15). Strikingly, these genes are expressed during and act in the formation of joints that form between the long bones by segmentation and in other classes of joints such as those between vertebrae and those between calvarial membranous bones. Different members of the Gdf family are expressed in diverse joints, and the loss of Gdf activity results in the failure of joint formation (16). In addition, β-catenin activity, a key effector of the canonical Wnt pathway, is required for joint formation, and ectopic *Wnt9a* is sufficient to initiate the formation of a joint interzone (9, 11, 17).

The condyle is an important growth site in the mandible with similarities to the growth plate of the long bones, and it displays four distinct zones: a fibrous cell layer, a progenitor cell layer, a zone of flattened chondrocytes, and a zone of hypertrophic chondrocytes (Fig. 1, upper right) (18, 19). One key gene previously noted to be expressed during and function within the growth plate of the condylar cartilage is *Indian hedgehog* (*Ihh*) (20–22). *Ihh* has been studied extensively during endochondral ossification of the long bones, where it plays several distinct roles. Secreted by prehypertrophic condrocytes that are just entering the differentiation pathway, Ihh is critical for maintaining the growth of adjacent proliferating chondrocytes. In addition, Ihh plays an indirect role in regulating the rate of chondrocyte differentiation by acting in a negative feedback loop with a second secreted protein, parathyroid-hormone-related protein (PTHrP), in the periarticular perichondrium. Chondrocytes within the range of PTHrP signaling are in turn blocked from entering the differentiation pathway. Thus, Ihh, in conjunction with PTHrP, plays a crucial role in organizing the growth plate (23–25). In potentially analogous fashion, in the absence of *Ihh*, the organization of the growth-plate-like zone in the TMJ condyle is disrupted, and the TMJ disk does not form (21). Ihh signals through its receptor Ptc1, itself a transcriptional target of Ihh. Acting through a second transmembrane protein, Smo, Ihh activity serves to regulate the processing and activity of the Gli family of transcription factors (26). Gli1 itself is transcriptionally up-regulated by Ihh signaling and is a transcriptional activator of

Author contributions: P.P. and C.J.T. designed research; P.P., B.W.J., and M.L.C. performed research; J.K.H. and P.V.T. contributed new reagents/analytic tools; P.P., D.J.O., R.L.M., and C.J.T. analyzed data; and P.P. and C.J.T. wrote the paper.

The authors declare no conflict of interest.

[1]To whom correspondence should be addressed. E-mail: tabin@genetics.med.harvard.edu.

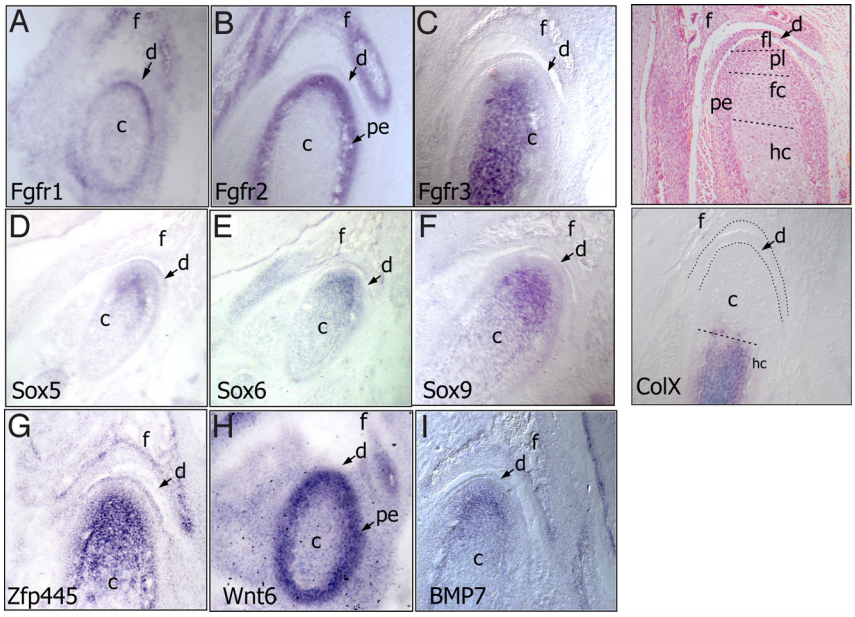

Fig. 1. RNA expression of *Fgfr1*, *Fgfr2*, *Fgfr3*, *Sox5*, *Sox6*, *Sox9*, *Zfp445*, *Wnt6*, and *BMP7* in mouse embryonic temporomandibular joint (TMJ). (*A–I*) In situ hybridization was performed on serial coronal cryosections of E16.5 TMJ. At this developmental stage, the mandibular condyle, temporal fossa, and TMJ disk are morphologically well defined. (*Upper right*) Different cell zones in the condyle. (*Lower right*) An in situ hybridization with *Collagen X* (*ColX*), a marker for hypertrophic chondrocytes. f, glenoid fossa of the temporal bone; c, condylar head of the mandible; d, joint disk; pe, perichondrium; fl, fibrous cell layer; pl, progenitor cell layer; fc, flattened chondrocytes; hc, hypertrophic chondrocytes.

Ihh targets. Gli3 acts predominantly as a transcriptional repressor and is down-regulated transcriptionally by Ihh signaling. Moreover, Ihh activity alters the processing of full-length Gli3 protein such that the repressor form is not produced. Finally, Gli2 functions mostly as a transcriptional activator, although in the absence of Ihh activity it retains some repressor function (27, 28). Functional Gli2 is necessary for normal endochondral bone development, as indicated in mice lacking the *Gli2* gene (29, 30), whereas in early limb development Gli3 is the only significant mediator of hedgehog (Hh) signaling (downstream of the Ihh-relative, Sonic hedgehog) (31). During skeletogenesis, the three Gli family members are active and exhibit some degree of functional redundancy in mediating Ihh signaling (27, 29).

In the present study, we sought to identify and further investigate genes that participate in TMJ development. Our observations indicate that the TMJ is unique not only structurally but also with respect to the expression of several key regulatory molecules. Furthermore, we analyzed the role of *Hh* signaling and found that it acts during at least two distinct steps in TMJ disk morphogenesis.

Results and Discussion

Identification of Genes Expressed in the TMJ. To identify genes expressed during the development of the major structures of the TMJ, we focused on tissues in the E16.5 mouse. At this stage, all of the distinct components of the TMJ have formed, but the joint is still in the process of maturation. The articular condyle and fossa were isolated separately by laser capture microdissection (LCM). The TMJ disk was included with the condyle sample. The RNA was extracted from the isolated tissues in triplicate and was subjected to microarray analysis. The E16.5 whole mouse was used as a reference sample. We found 3,035 probes enriched more than two-fold in the condyle sample with respect to the whole mouse reference and 1,465 probes enriched more than two-fold in the fossa. Genes with the highest signal intensities and fold enrichment were validated by in situ hybridization and selected for further analysis, with a particular focus on genes involved in known signaling pathways.

Consistent with the fact that both the condyle and fossa form by endochondral ossification, our array data showed the expression of many genes known to be involved in this process. For example, *FGF* and *FGF receptor* (*Fgfr*) gene families encode essential signaling molecules that function throughout all stages of bone development. *Fgfr1*, *Fgfr2*, and *Fgfr3* were highly expressed in our microarrays and were found by in situ analysis to be expressed in time-dependent and spatially restricted patterns. *Fgfr1* was expressed in the periosteum of the condyle and fossa, *Fgfr2* in the perichondrium of the condyle and fossa, and *Fgfr3* in the immature chondrocytes of the condyle [Fig. 1 *A–C* (32)]. The transcription factor *Sox9* was highly expressed in proliferating chondrocytes in the condyle at E16.5 and was down-regulated in hypertrophic chondrocytes (Fig. 1*F*). This finding is in agreement with the fact that *Sox9* is expressed in all chondroprogenitor cells and all chondrocytes and has an essential role in cartilage development (7, 33, 34). Expression of *Sox5* and *Sox6*, two transcription factors that act downstream of *Sox9* in other tissues, was seen in chondroprogenitor cells in a similar pattern as that of *Sox9*, indicating that the downstream role of Sox9 is conserved in the TMJ. However, their expression was weaker and more restricted, being localized toward the tip of the condyle (Fig. 1 *D* and *E*). A member of the SCAN (*S*RE-ZBP, *C*tfin51, *A*W-1, and *N*umber 18) family of zinc finger proteins of unknown function, Zfp445, also showed a very similar expression pattern to that of *Sox9* in chondroprogenitor cells. In addition, it was also expressed in disk and fossa at E16.5 (Fig. 1*G*). *Wnt6* and *BMP7* were detected in the microarray. Both genes have been shown previously to play important roles in limb joint development. *Wnt6* is particularly enriched in the perichondrium of the condyle, although it is also expressed in the chondroprogenitors (Fig. 1*H*). *BMP7* is found in the chondroprogenitor cells of the condyle (Fig. 1*I*).

In long bone development, Ihh signaling is known to indirectly negatively regulate the differentiation of chondrogenic precursor cells to mature chondrocytes and to mediate chondrocyte proliferation. We found the Hh pathway effector genes *Gli1*, *Gli2*, *Gli3*, their receptor *Ptch1*, and *Smo* among the highly enriched genes in the condyle by microarray analysis. Unexpectedly, none of the Hh ligands were enriched in our microarray data. To identify which Hh ligands are present in the TMJ, we tested for expression of the three known *Hh* ligand genes by in situ hybridization. Consistent with previous data (20, 21), *Ihh* was the only *Hh* detected in the mouse TMJ at E16.5, with high expression in the condylar prehypertrophic chondrocytes (Fig. 2*A*).

Because our LCM experiment was designed to interrogate specifically the tissues of the forming joint, these *Ihh*-expressing cells are located outside the boundaries of the microdissected region of the condyle, which likely explains the lack of *Ihh* signal in our microarray. Complementary to the *Ihh* expression pattern, *Gli1*, *Gli2*, *Gli3*, *Smo*, and *Ptc1* showed overlapping expression in the cartilage of the E16.5 mouse condyle (Fig. 2 *B–F*). At this

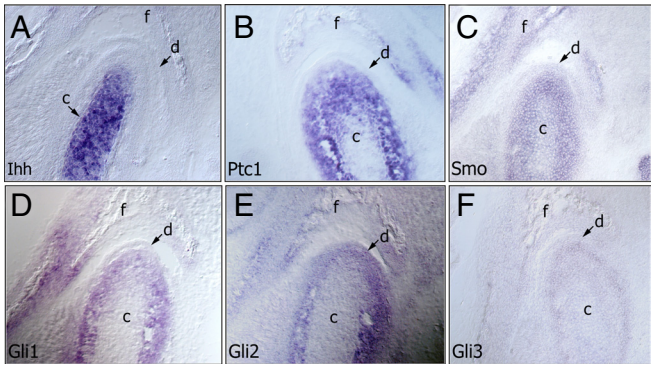

Fig. 2. RNA expression of *Ihh*, *Ptc1*, *Smo*, *Gli1*, *Gli2*, and *Gli3* in the mouse temporomandibular joint (TMJ). (*A–F*) Coronal cryosections of the TMJ at E16.5. In situ hybridization was performed for the indicated genes. Note high *Gli2* expression in disk joint. Ihh, Indian hedgehog; Ptc1, Patched 1; Smo, Smoothened; f, glenoid fossa of the temporal bone; c, condylar head of the mandible; d, joint disk.

embryonic stage, the *Gli2* expression was the strongest among the *Gli* genes, which together with *Smo* were the only genes in the Hh signaling pathway that were expressed at readily detectable levels in the joint disk (Fig. 2 *C* and *E*).

Comparison of Gene Expression in the TMJ and Other Synovial Joints. Most synovial joints develop by the cleavage or segmentation of a continuous skeletal condensation. However, the TMJ forms from separate condensations as the condylar blastema grows toward the temporal blastema until the gap between them closes (1). Gdf5, Gdf6, and Gdf7 are key factors expressed in the developing limb joints and between other skeletal elements (16). To see whether these key markers of limb synovial joints are also present during TMJ formation, we analyzed their expression in the mouse TMJ from E14 to E17 by in situ hybridization in parallel with E14 and E15 mouse limb joints as positive controls. Although they were expressed in limb joints, we could not detect their expression in the TMJ at the stages examined, nor were they enriched in our microarray data (Fig. 3 *A–C*, microarray data at National Center for Biotechnology Information).

Next, we sought to determine if TMJ development resembles that of two other synovial joints, the shoulder (gleno-humeral) and hip (ilio-femoral) joints, both of which form via separate condensations that grow toward one another, similar to the TMJ. We thus evaluated the expression of markers identified in our screen in these three joints at equivalent developmental stages. Development of the TMJ at E16.5 is nominally equivalent to E14.5 in the developing shoulder and hip joints. As shown in Fig. 3 *D* and *E*, *Gli1* and *Gli2* expression patterns were similar in the TMJ and the hip joint, whereas neither was clearly detectable in the shoulder joint. *Ihh* was highly expressed in the condyle of the TMJ adjacent to the joint but was expressed only at a distance from the other two joints (Fig. 3*F*). *Sox 5*, *Sox6*, *Sox9*, and *Zfp445* (Fig. 3 *G–J*) were strongly expressed at the tip of the head of the condyle in the TMJ but were absent from the fossa at this developmental stage. In contrast, these markers were expressed uniformly in the two bones comprising the other two joints.

TMJ Abnormalities in Gli2$^{zfd/zfd}$ Mutant Mice. *Gli2* was one of the most highly enriched genes in our screen. To define its functional role in TMJ formation, we examined mice homozygous for targeted disruption of the Gli2 zinc finger domain (Gli2$^{zfd/zfd}$), which abrogates the DNA binding function of the protein (30). *Gli2* mutants were compared with wild-type littermates (Fig. 4 *A* and *C*) at E16.5 and E18.5. Histological analysis of *Gli2*$^{-/-}$ mice showed that the TMJ disk was missing in these mice (Fig. 4 *B* and *D*). In addition, the condyle was much smaller in size, and the cellular organization

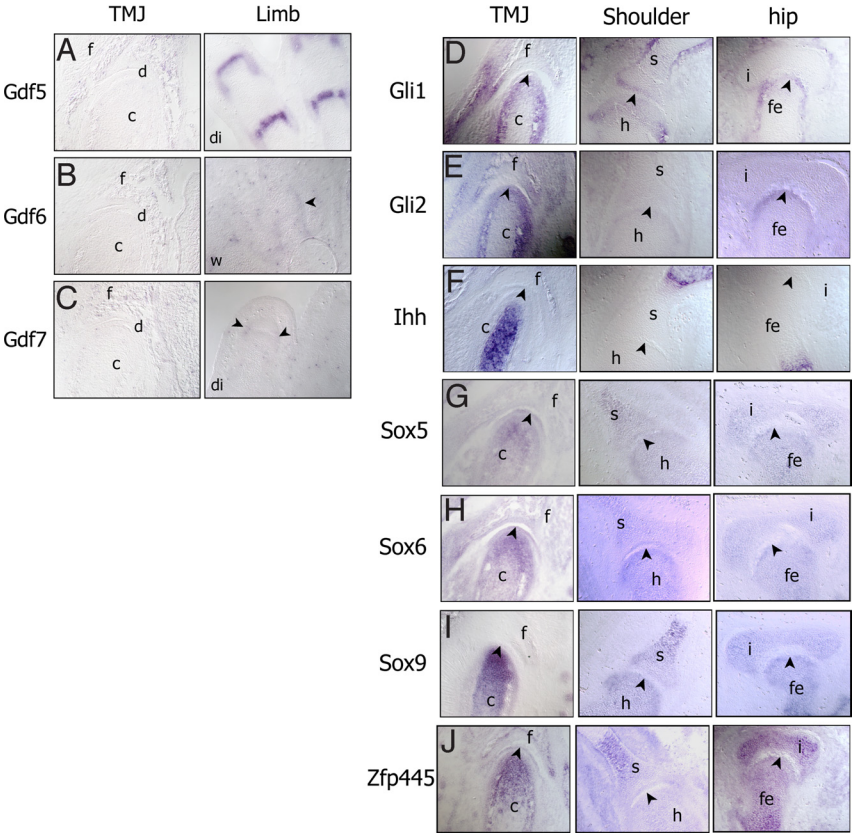

Fig. 3. Comparison of gene expression patterns between the temporomandibular joint (TMJ) and other developmentally matched synovial joints. Coronal sections of E16.5 TMJ and E14.5 limb (sagittal sections), shoulder (gleno-humeral), and hip joints (ilio-femoral). (*A–C*) *Gdf5*, *Gdf6*, and *Gdf7* in situ hybridization. Signal in limb was detected after 2 days, TMJ sections were left for 5 days, and no signal could be detected. *Gli1* (*D*), *Gli2* (*E*), *Ihh* (*F*), *Sox5* (*G*), *Sox6* (*H*), *Sox9* (*I*), and *Zfp445* (*J*). Arrowheads mark the location of each joint. f, glenoid fossa of the temporal bone; c, condylar head of the mandible; d, joint disk; w, wrist; di, digits; s, scapula; h, humerus; i, iliac bone; fe, femur.

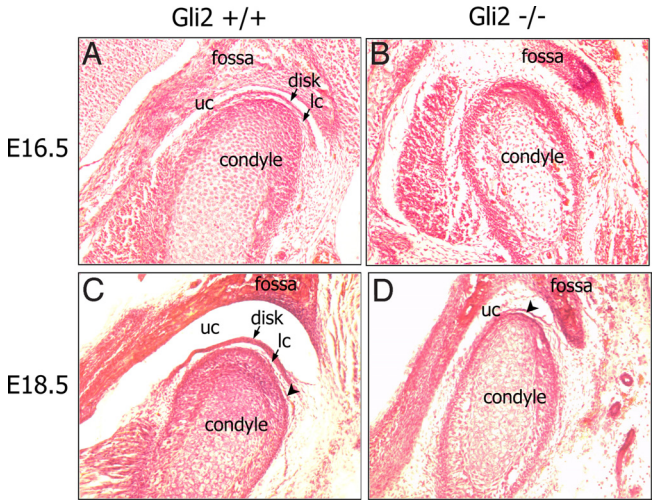

Fig. 4. Histological analysis of temporomandibular joint (TMJ) abnormalities in *Gli2*$^{-/-}$ embryos. (*A–D*) Serial coronal cryosections of E16.5 and E18.5 wild-type (*A*, *C*) and mutant mice (*B*, *D*). (A) Representative section through an E16.5 wild-type TMJ showing a well-defined condyle, glenoid fossa, and joint disk and distinguishable upper and lower synovial joint cavities. In the condyle, cells are smaller and in higher density in the apical region of the condyle and gradually increase in size and decrease in density toward the lower margin of the condyle. (*B*) Section through an E16.5 *Gli2*$^{-/-}$ TMJ. The condyle and fossa can be distinguished clearly, but no joint disk is noticeable. In addition, cells in the condyle are not organized as described in the wild-type littermate (*A*). (*C*) Section through an E18.5 wild-type TMJ showing well-defined condyle, glenoid fossa, and fibrous compact joint disk. Upper and lower joint cavities have enlarged. In the condyle, small cells are concentrated in the apical region, and the number of enlarged cells has increased. The perichondrium surrounding the condyle is wider and well defined. (*D*) Section through the TMJ of an E18.5 *Gli2*$^{-/-}$ mutant. Condyle, fossa, and upper joint cavity are evidently formed; however, the TMJ disk and lower joint cavity are not visible. Cells in the condyle appear disorganized, and the perichondrium is much thinner. Arrowheads in *C* and *D* indicate articular cartilage. uc, upper joint cavity; lc, lower joint cavity.

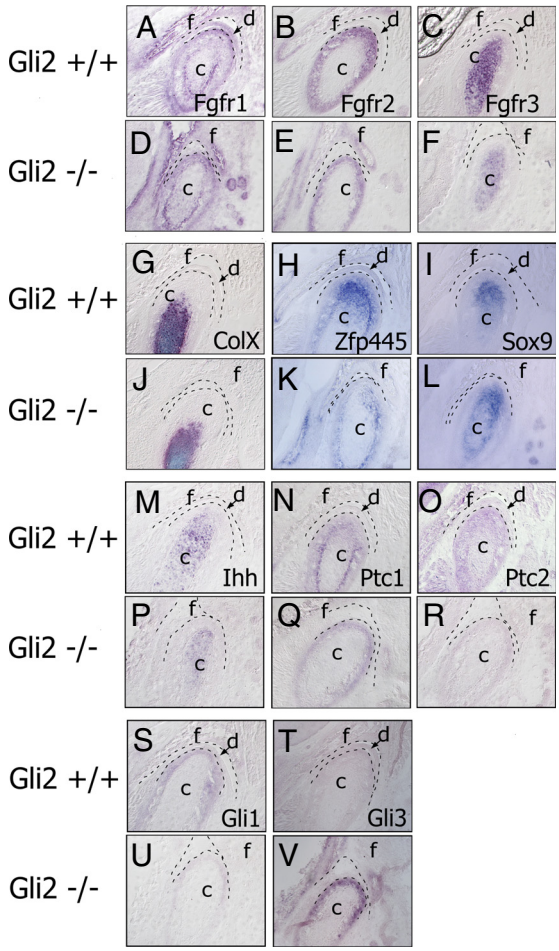

Fig. 5. Alterations in gene expression in *Gli2*$^{-/-}$ mouse temporomandibular joint (TMJ). (*A–V*) Serial coronal cryosections of the TMJ at E18.5 in wild-type and mutant (*Gli2*$^{-/-}$) mice. In situ hybridization was performed for the indicated genes. (*A*, *D*) *Fgfr1*, (*B*, *E*) *Fgfr2*, (*C*, *F*) *Fgfr3*, (*G*, *J*) *Collagen X* (*ColX*), (*H*, *K*) *Zinc finger protein 445* (*Zfp445*), (*I*, *L*) *Sox9*, (*M*, *P*) *Indian hedgehog* (*Ihh*), (*N*, *Q*) *Patched 1* (*Ptc1*), (*O*, *R*) *Patched 2* (*Ptc2*), (*S*, *U*) *Gli1*, and (*T*, *V*) *Gli3*. f, glenoid fossa of the temporal bone; c, condylar head of the mandible; d, disk. Dashed lines demarcate the boundaries of condyle and fossa.

of the growth plate within the condyle was lost. Moreover, cells at the growth plate appeared to be larger in size and disorganized (Fig. 4*B*). Additionally, chondroprogenitor cells and prehypertrophic chondrocytes were much reduced in number. We also analyzed mice at E18.5, just before birth, and found that the disk was also absent at that time point (Fig. 4*D*), therefore excluding the possibility that the lack of the disk in E16.5 mutant mice was due to a delay in the development of the TMJ. At E18.5, a distinct thin layer of cells can be discerned at the articular surface of the mutant condyle. On the basis of its morphology and because a similar structure distinct from the disk itself is present in wild-type littermates (Fig. 4 *C* and *D*, arrowheads), we interpret this as articular cartilage. At the present time, there is no specific marker for the TMJ disk, and therefore definitively distinguishing between articular cartilage and disk is not possible. However, the lack of a TMJ disk in *Gli2* mutants is in accord with observations in *Ihh*$^{-/-}$ mice (21). Thus, our experiments strongly suggest that the formation of the TMJ disk requires Gli2 activity. Interestingly, *Gli2* mutant mice also fail to develop intervertebral disks (29, 30), which are similar to the TMJ disk in that they consist of fibrocartilage. In a few instances, the TMJ disk was absent from one side of the mandible but was present or incompletely formed on the contralateral side, indicating that the *Gli2* mutation is not fully penetrant with respect to the TMJ phenotype. The reduction of proliferating chondrocytes in the *Ihh*$^{-/-}$ and *Gli2*$^{-/-}$ mutant condyles is consistent with the role of Ihh in maintaining the proliferating chondrocyte cell population and could account for the absence of disk formation in these mutants.

Molecular Analysis of Developing Condyle and Disk in *Gli2* Mutant Mice. To characterize further the condylar and disk defects arising in the absence of *Gli2*, we analyzed gene expression in serial sections of wild-type and *Gli2* mutant mice at E18.5. As shown in Fig. 5 *A* and *D*, *Fgfr1* expression remained unchanged in *Gli2* mutants compared with that in wild-type littermates. However, expression of *Fgfr2* and *Fgfr3* was much reduced in *Gli2* mutants. The perichondrium was significantly thinner in the mutants compared with that in wild-type littermates, as indicated by the lower *Fgfr2* expression. The lower expression of *Fgfr3* is consistent with the observation that immature chondrocytes were decreased significantly in number and density in the mutants (Fig. 5 *B*, *C*, *E*, and *F*). In long bones, *Gli2* is proposed to reduce proliferation via Fgf2 signaling and to inhibit hypertrophic differentiation by promoting signaling through Fgfr3. *Gli2*$^{-/-}$ and *Fgfr3* mutants show a similar phenotype (i.e., expansion of hypertrophic cells and *ColX*-positive chondrocytes in growth plates), suggesting that Gli2 acts upstream in the Fgfr3 signaling pathway to inhibit chondrocyte hypertrophy within the TMJ. Surprisingly, *ColX* expression did not increase in the *Gli2* mutant TMJ, even though there was an expansion in the number of enlarged chondrocytes (Fig. 5 *G* and *J*). Thus, in the absence of Gli2 activity, some aspects of chondrogenic differenti-

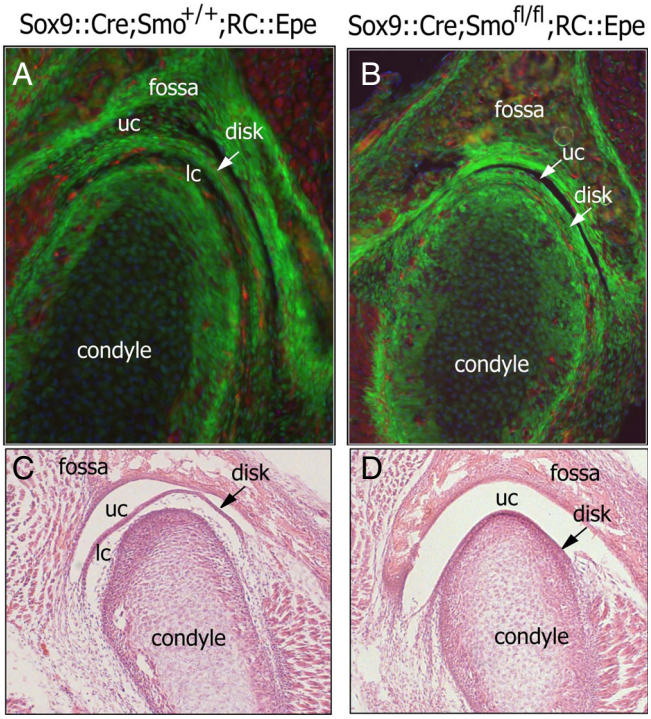

Fig. 6. Conditional ablation of *Smo* from chondroprogenitor cells. Cre recombinase activity in *Sox9*::*Cre* mice, using the GFP Cre reporter. The green GFP signal indicates cells in which Cre-Lox recombination has taken place, and the red cells represent expression of mCherry where Cre recombination did not occur. GFP and mCherry expression are mutually exclusive. (*A*) *Sox9*-expressing chondroprogenitor cells up to E17.5 are GFP-positive. Chondroprogenitor cells are distributed throughout the temporomandibular joint fossa, disk, and condyle. (*B*) GFP signal in an E17.5 *Sox9*::*Cre; Smo*$^{fl/fl}$;*RC*::*Epe* compound embryo. *Smo* was conditionally removed from *Sox9*-expressing cells. As a result, the condyle is much smaller than its wild-type counterpart, and the lower joint cavity (lc) is absent in the mutant (*A*, *B*). (*C*, *D*) Hematoxylin and eosin staining at E18.5 to visualize the loss of growth-plate-like organization in the condyle of the mutant (*D*) compared with its wild-type counterpart (*C*). uc, upper joint cavity.

ation are aberrant in the forming TMJ. Similarly, *Sox9* expression also was unchanged in the condyle despite a reduction in cells in the chondroprogenitor layer (Fig. 5 *I* and *L*). In contrast, *Zfp445*, which shows similar expression to *Sox9* in wild-type chondroprogenitor cells, was reduced dramatically in the *Gli2* mutant (Fig. 5 *H* and *K*). *Ihh*, *Ptc1*, *Ptc2*, and *Gli1* expression was reduced in the *Gli2* mutant; in contrast, *Gli3* was considerably up-regulated (Fig. 5 *M*–*V*). *Gli3* is well known to act as a repressor of *Sonic hedgehog (Shh)* and a repressor of osteoblastic bone formation. *Gli3* overexpression in the condyle of *Gli2* mutants possibly is contributing to the absence of TMJ disk formation. Gli proteins show partial functional redundancy in other tissues where they are coexpressed. Although *Gli1* and *Gli3* are expressed within the mutant TMJ, they are largely absent in the forming disk and are thus apparently unable to compensate for the lack of *Gli2* in TMJ disk development.

Hh Signaling Is Required at Two Distinct Steps in TMJ Disk Formation. In the absence of either *Gli2* (this work) or *Ihh* activity (20), the TMJ disk fails to form, and in the latter case, the process has been shown to be Gli3-independent (20). Interestingly, *Ihh* is expressed during early chondrogenesis within condensing mesenchymal cells, and in a potentially analogous fashion, both our observations and published data indicate that *Ihh* is expressed in the TMJ condyle during early mesenchymal condensation before disk formation [approximately E13.5 (22)]. These observations suggest that Hh signaling through *Gli2* could act very early in inducing disk differentiation. Alternatively, because *Gli2* continues to be expressed within the disk after it has undergone chondrogenic differentiation and initiated *Sox5*, *Sox6*, and *Sox9* expression (Fig. 1), *Hh* could be required at a later stage to maintain the disk.

To examine these possibilities, we conditionally removed *Smo* activity, required for Hh signaling, after cells have initiated chondrogenesis using a Cre allele under the control of the *Sox9* promoter. *Sox9*::*Cre; Smo*$^{fl/fl}$ and *Sox9*::*Cre; Smo*$^{+/+}$ control mice were constructed in a background carrying a GFP reporter for Cre activity at the Rosa26 locus (*RC*::*Epe*, B. Seri and S. M. Dymecki, Harvard Medical School, Boston, MA, personal communication). This reporter irreversibly activates GFP expression after exposure to Cre recombinase such that any cell derived from one that expressed Cre will be green. With this allele, any cell in which Cre-mediated recombination has not occurred expresses mCherry and hence is red. The expression of GFP and mCherry is mutually exclusive. As expected in the E17.5 TMJ, the condyle, fossa, and disk are GFP-positive, indicating that they consist of cartilage or descend from cells of the chondrogenic lineage. The condyle of the mutant progeny, *Sox9*::*Cre; Smo*$^{fl/fl}$; *Re*::*Epe*, was smaller in size and exhibited abnormal cellular organization with respect to control littermates, similar to *Gli2* mutants (Fig. 6 *C* and *D*).

Remarkably, the mutant TMJ formed a complete disk with a similar morphology to that seen in wild-type animals (Fig. 6 *A* and *B*). However, the disk forms in close proximity to the condyle, and as a consequence there is an absence of the lower joint cavity. Notably, the upper joint cavity is of approximately normal size. The failure of the disk to separate from the condyle is not a developmental delay, because the lower joint cavity fails to form even at later stages of development (Fig. 6 *C* and *D*).

Taken together, these data suggest that *Hh* signaling is required to initiate TMJ disk formation, as evident from disk agenesis or absence in both *Ihh* and *Gli2* mutants. We also discovered that *Hh* is required at a later step, after chondrogenic differentiation and *Sox9* expression commence, in order for the disk to undergo proper morphogenesis and form the joint cavity (See model in Fig. 7). The alternative possibility—that the mutant condyle grows into the joint cavity—is unlikely, because the entire condyle is smaller in the mutant relative to that in the wild type.

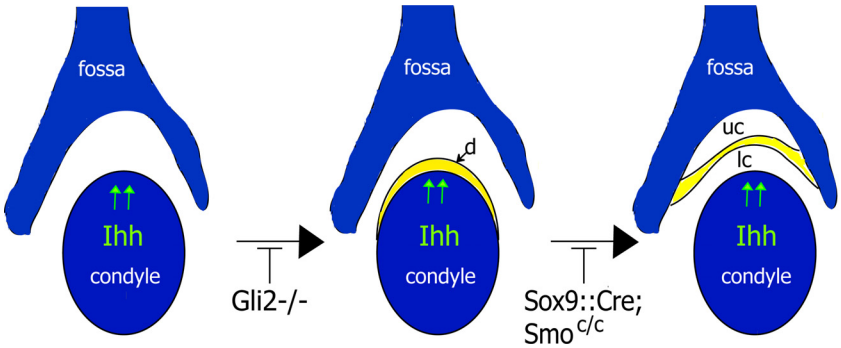

Fig. 7. Model for the requirement of hedgehog in temporomandibular joint formation. Indian hedgehog (Ihh) is localized in prehypertrophic chondrocytes in the condyle and required for disk induction. In the absence of Gli2, there is no disk (d) induction. Disk separation and lower joint cavity (lc) formation are inhibited after the removal of Smo from Sox9-expressing cells. uc, upper joint cavity.

In summary, our data indicate that the TMJ is a unique synovial joint not only in terms of its structure but also in terms of the developmental genetic pathways that govern its formation. Of particular interest, the TMJ disk forms in a two-step process, both of which are dependent upon *Hh* signaling. The first step involves disk formation, followed by subsequent stages of disk maturation that culminate in separation from the condyle to form the lower joint cavity. Future studies will need to investigate the relationship between *Hh* and other genes involved in the growth and differentiation of chondrocytes and how they affect the ability of the disk to separate from the condyle. A better understanding of TMJ organogenesis will allow the development of tools that can be used for the ex vivo synthesis of the relevant tissues and that can be used potentially in therapeutic approaches for TMJ disorders.

Methods

Embryo Collection and Mouse Genotyping. All animal procedures were performed according to guidelines approved by the Harvard Medical Area Institutional Animal Care and Use Committee.

The generation and genotyping of *Gli2* mutant mice was as described in ref. 29. Heterozygous $Gli2^{+/-}$ mice in F1 mixed backgrounds (C3H/HeJ: Fvb/N) were mated to generate homozygous $Gli2^{-/-}$ embryos. We analyzed six E16 mutant embryos and eight E18 mutant embryos. $Smo^{fl/fl}$ mice (35) were obtained from *JAX* and were mated with *RC*::$Epe^{+/+}$. $Smo^{fl/fl}$; *RC*::$Epe^{+/+}$ mice were generated subsequently by intercrossing between $Smo^{fl/+}$; *RC*::$Epe^{+/-}$ siblings. *Sox9*::*Cre* knock-in mice (36) were mated with mice homozygous for the floxed *Smo* alleles. The offspring inheriting both the Cre-recombinase gene and the floxed allele then were mated with $Smo^{fl/fl}$ or $Smo^{fl/fl}$; *RC*::$Epe^{+/+}$ to obtain embryos with the $Smo^{fl/fl}$ and the *Sox9*::*Cre* knock-in allele. Routine mouse genotyping was performed by PCR. The following primer pairs were used: floxed *Smo* allele (5′-CCACTGCGAGCCTTTGCGCTAC-3′ and 5′-AAGAACTCGTCAAGAAGGCGATAGAAGGCG-3′), wild-type *Smo* allele (5′-CCACTGCGAGCCTTTGCGCTAC-3′ and 5′-CCCATCACCTCCGCGTCGCA-3′), and *Sox9-Cre* knock-in allele (5′-GCAGAACCTGAAGATGTTCGC-3′ and 5′-ACACCAGAGACGGAAATCCATC-3′). Noon of the day of vaginal plug discovery was designated as E0.5.

Sample Collection, Laser Capture Microdissection, RNA Purification, and Microarray Analysis. The E16.5 CD1 mouse embryonic heads were rapidly dissected from embryos, rinsed in cold PBS, embedded in OCT compound (Tissue-Tek), and stored at −80 °C until sectioning. The 8-μm cryosections were collected on Arcturus PEN membrane glass slides (Molecular Devices). Laser capture microdissection was performed with an Arcturus Veritas instrument using CapSure HS LCM caps (Molecular Devices). Independent total RNA preparations were made from laser-captured condyle articular region, including the joint disk, and from the articular region of the fossa, using the PicoPure RNA isolation kit (Molecular Devices). Briefly, total RNA was extracted from approximately 1,000 captured cells by incubating LCM caps in extraction buffer. The RNA was amplified using RiboAmp HS RNA amplification kit (Molecular Devices). Five micrograms of cDNA from each sample was used to hybridize with Affymetrix GeneChip mouse genome array 430 2.0. For a reference sample, E16.5 whole mouse embryos were used to purify RNA, and 5 μg of cDNA was used for Affymetrix GeneChip hybridization. Microarray analyses were carried out using the Bioconductor and GeneSifter programs. Each experiment was done in triplicate. Microarray data is accessible at http://www.ncbi.nlm.nih.gov/geo/query/acc.cgi?acc=GSE17473.

Histological Analyses. For the histological analysis, E14.5–E19.5 embryos were decapitated, and heads and bodies were fixed separately in 4% paraformaldehyde and embedded in paraffin. Ten-micrometer sections were stained with hematoxylin and eosin following standard procedures.

Gene Expression. In situ hybridization was performed as described in ref. 37 on 16-μm cryosections using digoxigenin (DIG)-labeled probes. The DIG-labeled probes were detected with BM purple (Roche). The following mouse probes were used: *Fgfr1*(≈3.6 kb), *Fgfr2* (≈900 bp), *Sox5* (488 bp), *Sox6* (481 bp), *Sox9* (255 bp), *Wnt6* (≈1.6 kb), *Bmp7* (≈2.1 kb), *Gdf5* (551 bp), *Gdf6* (481 bp), *GDF7* (478 bp), *Ihh* (700 bp), *Ptc1* (406 bp), *Ptc2* (2 kb), *Gli1* (≈800bp), *Gli2* (≈1 kb), *Gli3* (≈400bp), and *ColX* (≈650 bp). Probes made by RT-PCR product used the following primers: *Fgfr3* (5′-CGCATCCTCACTGTGACATC-3′ and 3′-GGAAATGAGAGGGCCAGAAC-5′), *Smo* (5′-AGAGCAAGATGATCGCCAAG-3′ and 3′-ATCCAAGATCTCAGCCTCCA-5′), and *Zfp445* (5′-GCGTGGGTAGAAAAAGGCTA-3′, 3′-CTCATCCCGGTCTGTCAAAT-5′).

For fluorescent signal visualization on sections, tissues were fixed for 2–4 h in 4% paraformaldehyde and cryoembedded, and 10-μm sections were collected. Pictures were captured on a Zeiss AxioImager Z1 microscope with an AxioCam HRm camera.

ACKNOWLEDGMENTS. We thank Drs. Alexandra L. Joyner (Memorial Sloan-Kettering Cancer Center, New York, NY) for providing the $Gli2^{zfd/zfd}$ mice, Susan M. Dymecki (Harvard Medical School, Boston, MA) and Bettina Seri (Harvard Medical School, Boston, MA) for providing *RC*:: *Epe* mice, Rahul N. Kanadia (Harvard Medical School, Boston, MA) and Philip P. Stashenko (The Forsyth Institute, Boston, MA) for helpful suggestions and discussion. This work was supported by the National Institute of Dental and Craniofacial Research Award K22DE-016309 (to P.P.) and Grant P01 DK56246 (to C.J.T.) and the Children's Hospital Pathology Foundation with funds from the S. Burt Wolbach Chair in Pathology (M.L.C.). This manuscript is dedicated to the memory of Dr. Tucker Collins, whose equipment and expertise in laser capture microscopy, and whose generosity and passion for science were essential to this study.

1. Avery JK (2001) *Oral Development and Histology* (Thieme, New York) 3rd Ed, p 435.
2. Hinchliffe JR and Johnson DR (1980) *The Development of the Vertebrate Limb* (Clarendon, Oxford).
3. Shubin NH, Alberch P (1986) A morphogenetic approach to the origin and basic organization of the tetrapod limb. *Evol Biol* 20:319–387.
4. Oster GF, Shubin N, Murray JD, Alberch P (1988) Evolution and morphogenic rules: The shape of the vertebrate limb in ontogeny and phylogeny. *Evolution* 42:862–884.
5. Craig FM, Bentley G, Archer CW (1987) The spatial and temporal pattern of collagens I and II and keratan sulphate in the developing chick metatarsophalangeal joint. *Development* 99:383–391.
6. Khan IM, et al. (2007) The development of synovial joints. *Curr Top Dev Biol* 79:1–36.
7. Akiyama H, Chaboissier MC, Martin JF, Schedl A, de Crombrugghe B (2002) The transcription factor Sox9 has essential roles in successive steps of the chondrocyte differentiation pathway and is required for expression of Sox5 and Sox6. *Genes Dev* 16:2813–2828.
8. Ikeda T, et al. (2005) Distinct roles of Sox5, Sox6, and Sox9 in different stages of chondrogenic differentiation. *J Bone Miner Metab* 23:337–340.
9. Hartmann C, Tabin CJ (2001) Wnt-14 plays a pivotal role in inducing synovial joint formation in the developing appendicular skeleton. *Cell* 104:341–351.
10. Später D, Hill TP, Gruber M, Hartmann C (2006) Role of canonical Wnt-signalling in joint formation. *Eur Cell Mater* 12:71–80.
11. Später D, et al. (2006) Wnt9a signaling is required for joint integrity and regulation of *Ihh* during chondrogenesis. *Development* 133:3039–3049.
12. Storm EE, Kingsley DM (1996) Joint patterning defects caused by single and double mutations in members of the bone morphogenetic protein (BMP) family. *Development* 122:3969–3979.
13. Storm EE, Kingsley DM (1999) GDF5 coordinates bone and joint formation during digit development. *Dev Biol* 209:11–27.
14. Wolfman NM, et al. (1997) Ectopic induction of tendon and ligament in rats by growth and differentiation factors 5, 6, and 7, members of the TGF-β gene family. *J Clin Invest* 100:321–330.
15. Francis-West PH, et al. (1999) Mechanisms of GDF-5 action during skeletal development. *Development* 126:1305–1315.
16. Settle SH, Jr, et al. (2003) Multiple joint and skeletal patterning defects caused by single and double mutations in the mouse Gdf6 and Gdf5 genes. *Dev Biol* 254:116–130.
17. Guo X, et al. (2004) Wnt/β-catenin signaling is sufficient and necessary for synovial joint formation. *Genes Dev* 18(19):2404–2417.
18. Sarnat BG (1966) Developmental facial abnormalities and the temporomandibular joint. *Dent Clin North Am* Nov:587–600.
19. Silbermann M, Frommer J (1972) The nature of endochondral ossification in the mandibular condyle of the mouse. *Anat Rec* 172:659–667.
20. Tang GH, Rabie AB, Hagg U (2004) Indian hedgehog: A mechanotransduction mediator in condylar cartilage. *J Dent Res* 83:434–438.
21. Shibukawa Y, et al. (2007) Temporomandibular joint formation and condyle growth require Indian hedgehog signaling. *Dev Dyn* 236:426–434.
22. Gu S, Wei N, Yu L, Fei J, Chen Y (2008) Shox2-deficiency leads to dysplasia and ankylosis of the temporomandibular joint in mice. *Mech Dev* 125:729–742.
23. Lanske B, et al. (1996) PTH/PTHrP receptor in early development and Indian hedgehog-regulated bone growth. *Science* 273:663–666.
24. Vortkamp A, et al. (1996) Regulation of rate of cartilage differentiation by Indian hedgehog and PTH-related protein. *Science* 273:613–622.
25. St-Jacques B, Hammerschmidt M, McMahon AP (1999) Indian hedgehog signaling regulates proliferation and differentiation of chondrocytes and is essential for bone formation. *Genes Dev* 13:2072–2086.
26. Ingham PW, McMahon AP (2001) Hedgehog signaling in animal development: Paradigms and principles. *Genes Dev* 15:3059–3087.
27. Bai CB, Joyner AL (2001) Gli1 can rescue the in vivo function of Gli2. *Development* 128:5161–5172.
28. Wang B, Fallon JF, Beachy PA (2000) Hedgehog-regulated processing of Gli3 produces an anterior/posterior repressor gradient in the developing vertebrate limb. *Cell* 100:423–434.
29. Mo R, et al. (1997) Specific and redundant functions of Gli2 and Gli3 zinc finger genes in skeletal patterning and development. *Development* 124(1):113–123.
30. Miao D, et al. (2004) Impaired endochondral bone development and osteopenia in Gli2-deficient mice. *Exp Cell Res* 294:210–222.
31. Hui CC, Joyner AL (1993) A mouse model of greig cephalopolysyndactyly syndrome: The *extra-toes*^{J} mutation contains an intragenic deletion of the *Gli3* gene. *Nat Genet* 3:241–246.
32. Rice DP, Rice R, Thesleff I (2003) Fgfr mRNA isoforms in craniofacial bone development. *Bone* 33:14–27.
33. Ng LJ, et al. (1997) SOX9 binds DNA, activates transcription, and coexpresses with type II collagen during chondrogenesis in the mouse. *Dev Biol* 183:108–121.
34. Zhao Q, Eberspaecher H, Lefebvre V, De Crombrugghe B (1997) Parallel expression of Sox9 and Col2a1 in cells undergoing chondrogenesis. *Dev Dyn* 209:377–386.
35. Long F, Zhang XM, Karp S, Yang Y, McMahon AP (2001) Genetic manipulation of hedgehog signaling in the endochondral skeleton reveals a direct role in the regulation of chondrocyte proliferation. *Development* 128:5099–5108.
36. Akiyama H, et al. (2005) Osteo-chondroprogenitor cells are derived from Sox9 expressing precursors. *Proc Natl Acad Sci USA* 102:14665–14670.
37. Brent AE, Schweitzer R, Tabin CJ (2003) A somitic compartment of tendon progenitors. *Cell* 113:235–248.